

# UC Davis

## UC Davis Previously Published Works

### Title

Osteogenic benefits of low-intensity pulsed ultrasound and vibration in a rodent osseointegration model.

### Permalink

<https://escholarship.org/uc/item/1tw99576>

### Journal

Journal of musculoskeletal & neuronal interactions, 19(2)

### ISSN

1108-7161

### Authors

Ruppert, David S  
Harrysson, Ola LA  
Marcellin-Little, Denis J  
[et al.](#)

### Publication Date

2019-06-01

Peer reviewed

## Original Article

# Osteogenic benefits of low-intensity pulsed ultrasound and vibration in a rodent osseointegration model

David S. Ruppert<sup>1</sup>, Ola L.A. Harrysson<sup>1,3</sup>, Denis J. Marcellin-Little<sup>1,3,4</sup>, Seth Bollenbecker<sup>5</sup>, Paul S. Weinhold<sup>1,2</sup>

<sup>1</sup>Department of Biomedical Engineering, UNC-NCSU; <sup>2</sup>Department of Orthopaedics, School of Medicine, UNC; <sup>3</sup>Edward P. Fitts Department of Industrial and Systems Engineering, NCSU; <sup>4</sup>Department of Clinical Sciences, College of Veterinary Medicine, NCSU; <sup>5</sup>Department of Biology and Chemistry, School of Medicine, UNC

## Abstract

**Objectives:** Osseointegrated prostheses are increasingly used for amputees, however, the lengthy rehabilitation time of these prostheses remains a challenge to their implementation. The aim of this study was to investigate the ability of locally applied vibration or low-intensity pulsed ultrasound (LIPUS) to accelerate osseointegration and increase peri-implant bone volume. **Methods:** A 4-week and 8-week rodent study were conducted in a femoral intramedullary implant model (control, vibration, LIPUS, and combined treatment) to determine effects on healing. Osseointegration was evaluated quantitatively through mechanical,  $\mu$ CT and histological evaluations. **Results:** Maximum pushout load at 4 weeks increased with LIPUS relative to control (37.7%,  $P=0.002$ ). Histologically, LIPUS and vibration separately increased peri-implant bone formation after 4 weeks relative to control. Vibration resulted in greater peri-implant bone after 8 weeks than all other groups (25.7%,  $P<0.001$ ). However, no significant group differences in pushout load were noted at 8 weeks. **Conclusions:** Although vibration increased bone around implants, LIPUS was superior to vibration for accelerating osseointegration and increasing bone-implant failure loads at 4 weeks. However, the LIPUS benefits on osseointegration at 4 weeks were not sustained at 8 weeks.

**Keywords:** Low-Intensity Pulsed Ultrasound, Vibration, Bone-Implant Interface, Osseointegration, Intramedullary Implant

## Introduction

In 2005, the prevalence of amputees in the United States was ~1 in 190<sup>1</sup>. That prevalence is expected to double by 2050. Direct skeletal attachment of limb prostheses via percutaneous osseointegrated implants is an emerging alternative to socket prostheses, with several advantages that improve overall quality of life<sup>2</sup>; especially for patients with short residuum and high soft-tissue volume<sup>3</sup>. Implants directly connected to living bone in amputated limbs allows

for a more stable connection enabling greater control of the prosthesis and heightened osseoperception (sensory feedback from the environment)<sup>4</sup> while eliminating problems associated with socket-devices such as painful skin lesions and irritations<sup>5</sup>.

Direct osseointegration of metal implants has been shown to be a viable long-term solution for connection to the skeletal system but requires reduced loads during the healing period<sup>3,6,7</sup>. Implant coatings and metal porosity are being studied to reduce infection and promote osseointegration<sup>8,9</sup>. However, fibrous encapsulation of osseointegrated implants still occurs, impairing long-term implant stability<sup>10,11</sup>. Premature loading of osseointegrated implants before complete bone-implant osseointegration can lead to excessive micromotion<sup>12,13</sup> which in turn may result in fibrous ingrowth instead of bone ingrowth<sup>14</sup>. To avoid fibrous ingrowth into the implant resulting from excessive loading and micromotion, controlled and gradual rehabilitation occurs over a 12-month period<sup>15</sup>. It is critical to identify methods of accelerating osseointegration and therefore to

The authors have no conflict of interest.

Corresponding author: David S. Ruppert, MSME, University of North Carolina, Orthopaedic Research Labs, CB# 7546, 134 Glaxo Bldg., 101A Mason Farm Rd, Chapel Hill, NC 27599  
E-mail: dsrupper@ncsu.edu

Edited by: G. Lyritis

Accepted 20 February 2019



shortening the rehabilitation period while also lessening the likelihood of fibrous ingrowth.

Low-magnitude, high-frequency (LMHF) whole body vibration (WBV) and low-intensity pulsed ultrasound (LIPUS) are two methods that show promise for accelerating osseointegration. Previous studies investigating fracture healing have indicated that both therapies are beneficial to bone healing through mechanisms not clearly defined<sup>16-18</sup>. The range of in WBV amplitudes that stimulate osseointegration has been reported<sup>19,20</sup>. Local application of vibration has not been previously investigated as a means of accelerating intramedullary implant osseointegration. However, local application of vibration may be preferable to WBV clinically in order to reduce the risk of adverse responses that might occur with whole body exposure such as back pain and Raynaud's syndrome<sup>21</sup>. In the current study, an optimal vibration amplitude of 0.6 g peak acceleration identified in an earlier WBV study was used as the basis for locally applied vibration.

While past studies have shown LIPUS is able to accelerate osseointegration in transverse implantation models<sup>22,23</sup>, it is unclear whether sufficient stimulus can reach the endosteal surfaces to improve implant stability in a more clinically relevant intramedullary implantation model<sup>24</sup>. Therefore, an intramedullary implant model was used in this study to evaluate the efficacy of LIPUS treatment in accelerating osseointegration.

The combined effect of locally applied vibration and LIPUS on osseointegration has not been previously investigated, and thus, these therapies were combined in this study to determine if their potential stimulatory effects on osseointegration were additive.

The objective of this study was to determine if locally applied LMHF vibration or LIPUS would accelerate osseointegration of the bone-implant interface and improve peri-implant bone volume at 4 and 8 weeks. We hypothesized that each therapy would improve osseointegration and peri-implant bone volume and that when the therapies were combined their effects on osseointegration would be additive.

## Materials and methods

A 4-week-long *in vivo* study was performed to determine early osseointegration characteristics of control, LIPUS and local vibration in a bilateral intramedullary femoral implant model. A subsequent 8-week study was conducted to determine further osseointegration and the combined effects of the treatments. Bone ongrowth was evaluated using mechanical pushout,  $\mu$ CT and histomorphometry for both studies. All animal work was carried out in accordance to the Animal Research: Reporting of *In-Vivo* Experiments (ARRIVE) guidelines and approved by the local Institutional Animal Care and Use Committee (IACUC). Female retired breeder (mean age= 24 weeks) Sprague-Dawley rats (Charles River Laboratories, Wilmington, MA) were given *ad libitum* access to food and water with a 12-hr light/dark cycle (7AM – 7PM).

Based on previous intramedullary implantation rat studies<sup>25</sup>, a standard deviation of 25% of the mean pushout strength was estimated. To detect a 40% difference in strength between the 3 treatment groups of the 4-week study with a power of 0.80 and an alpha of 0.05, power analysis calculated an N of 9 rats. To compensate for the potential loss of animals due to surgical complications, each group included 10 rats. The power analysis calculated an N of 10 rats to detect the same difference in strength between the four treatment groups of the 8-week study. Due to confidence in surgical outcomes achieved during the 4-week study, each group included 10 rats. Based on previous experience with  $\mu$ CT results<sup>26</sup>, an N of 8 and 9 for the 4 and 8-week studies respectively was calculated using the prior power analysis with a detectable difference of 35% and standard deviation of 20%.

### Implant model

Biocompatible, grade 5 titanium, 20-mm-long and 1.5-mm-diameter implants were fabricated with a 1.6-mm boss on their last 1.5 mm and a dimple in each end to facilitate surgical implantation and mechanical pushout<sup>26</sup>. The implants were additively manufactured, textured by acid etching, optically evaluated and handled identically to the intramedullary implants of a prior study<sup>26</sup>. The implants had a mean  $\pm$  SD surface roughness<sup>25</sup> of Ra= 10 $\pm$ 0.3  $\mu$ m.

### Surgical model

On the day of surgery, each rat received bilateral femoral implants. The distal femurs were exposed as described previously<sup>27</sup>. An 18-gauge needle was used to start a hole in the intercondylar notch while the final hole was reamed and extended to a 21-mm depth manually with a 1.5-mm twist bit without irrigation<sup>28</sup>. The implant was inserted by manual thrust and torque into the drilled hole until flush with the articular surface. The joint capsule was closed with 4-0 polyglactin 910 suture<sup>29</sup>. The incision was closed using wound clips (Autoclips, MikRon Precision Inc, Gardena, CA) and tissue adhesive (TA5, Med Vet International, Mettawa, IL). Each rat was given a subcutaneous injection of 0.5 mg/kg buprenorphine SR and 0.15 mL ceftriaxone preoperatively for amelioration of postsurgical pain and to prevent infection, respectively. A 5-mL lactated ringer's subcutaneous injection was given to each animal following surgery. A 1.6 mg/mL acetaminophen solution was provided *ad libitum* for seven days post-surgery. Radiographs were acquired 12 days after surgery to confirm proper implant placement and thereupon wound clips were removed.

### Treatments

A dual-limb local vibration stimulator was constructed from a pair of electromagnetic minishakers (Brüel & Kjær, Nærum, Denmark), a signal generator and an amplifier. The output amplitude of the local 45 Hz vibration system was tuned so the magnitude of vibration at the femur matched the

0.6 g peak acceleration for the optimal *in vivo* WBV amplitude of prior work<sup>19</sup>.

After implantation surgeries, animals in the 4-week study were randomly divided into three groups: control, LIPUS, and LMHF vibration to maintain uniform mean body weights between groups. Animals in the 8-week study were divided into four groups: control, LIPUS, vibration, and combined LIPUS/vibration as applied above. Treatments were started seven days after surgery and rats received treatment 20 min per day, five days per week<sup>25</sup>. All animals were secured in a custom rat restraint system while under isoflurane inhalation induced anesthesia and then allowed to awaken to position the knees in a flexed and externally rotated presentation (Figure 1). Once conscious, the designated 20-minute treatment was initiated (control, vibration or LIPUS). The vibration stimulus was directly applied bilaterally to the knee joints, minimizing dampening effects from surrounding soft tissue. A LIPUS applicator (Exogen 4000+, Bioventus, Durham, NC) was centered over the approximated mid-point of the implant on each limb. Neither LIPUS nor locally applied vibration has been approved by the FDA for this therapy mode. The control was secured with a polyacetal disc for 20 minutes simulating the LIPUS applicator. Rats quickly became accustomed to the restraint and struggled minimally (<2 min) during the initial days of treatment. At the completion of each treatment, rats were removed from restraints, returned to their cage and fed a sweetened cereal (Froot Loops, Kellogg's, Battle Creek, Michigan, US) to reduce stress post restraint and prevent stress-associated weight loss<sup>30,31</sup>.

After the 4 and 8 week rehabilitation periods, the animals were humanely euthanized by CO<sub>2</sub> overdose followed by thoracotomy. The right femurs were collected, wrapped in saline soaked gauze and stored at -20°C until mechanical testing. The contralateral limb, used for  $\mu$ CT and histology, was fixed in 70% ethanol at the time of dissection.

#### Mechanical testing

Mechanical push-out testing, evaluating the bone-implant stiffness; maximum load to bone-implant failure; and energy to failure, was performed to assess osseointegration as done in a prior study<sup>26</sup>. The proximal femur was removed to allow pushout of implants and the residual specimen potted using a self-curing acrylic resin (Ortho Jet BCA, Lang Dental, Wheeling, IL) as previously described<sup>26</sup>.

Mechanical testing was carried out with a material testing system (MTS) (8500 Plus, Instron Corp., Norwood, MA). The linear load of the MTS was transferred to the implant through a tapered stainless steel pin and measured with a 1kN load cell. Specimens were preloaded to 5 N and pushed at a constant rate of 2 mm/min until failure of the bone-implant interface.

#### Ex-vivo $\mu$ CT

Osseointegration was evaluated by bone volume fraction (BV/TV) along a 2.5 mm length, 2 mm from the proximal end

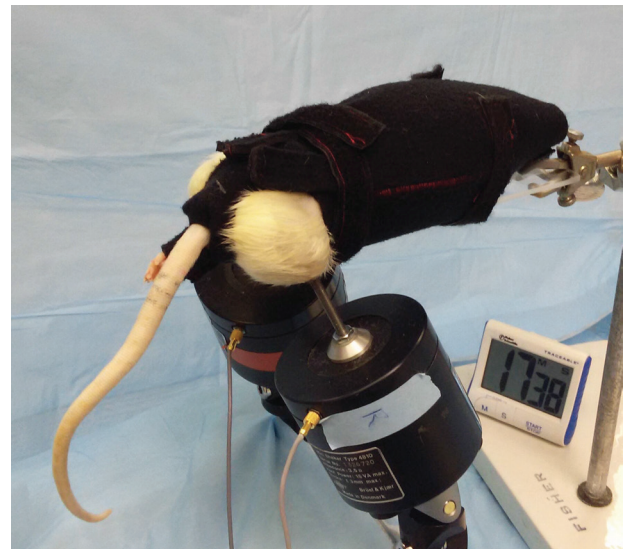


**Figure 1.** Rat in custom restraint system undergoing locally applied vibration treatment.

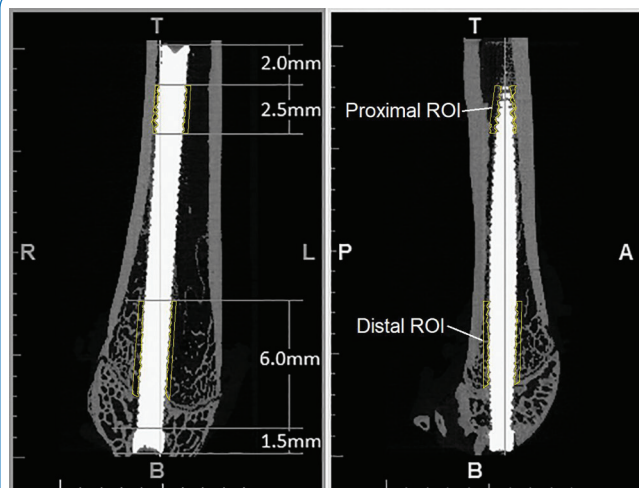


**Figure 2.** Regions of interest for  $\mu$ CT evaluation of bone volume fraction (BV/TV) in a predominantly cortical region versus a cancellous region.

and along 6 mm, 1.5 mm from the distal end of the implant (Figure 2) using  $\mu$ CT to assess a predominantly cortical region versus a cancellous bone region, respectively<sup>32</sup>. Femurs were scanned on equipment (40 model specimen CT, Scanco Medical, Brüttisellen, Switzerland) with settings (70 kVp, 114  $\mu$ A, and 8 W) as described<sup>33</sup> with a 10-mm field of view on "medium resolution" with a cubic voxel size of 12  $\mu$ m. The proximal end of the femur of each specimen was removed using a fine-toothed rotary bone saw 1 mm proximal to the



**Figure 3.** Digital image of acid fuchsin stained section of femur for histomorphometric evaluation.

implant to facilitate placement in the  $\mu$ CT x-ray tube as well as subsequent infiltration of methacrylate resin.

The  $\mu$ CT scans were analyzed using medical image processing software (Mimics 16.0, Materialise, Plymouth, MI). The implant was dilated by five pixels (60  $\mu$ m) to exclude the metal-induced artifact as determined previously<sup>33</sup>. The bone was segmented out using low and high thresholds of 529 and 1615 mg HA/cm<sup>3</sup>, respectively. Implants were segmented using a threshold  $\geq 2249$  mg HA/cm<sup>3</sup>.

The BV/TV within 250  $\mu$ m of the implant was calculated<sup>20</sup>. Due to a distinct cortical shell seen in the proximal scans, the cortical shell was excluded from BV/TV calculations (Figure 2). However, the cortical region near the epiphyseal line was less distinct and was included in analyses of the distal regions. BV/TV calculations were limited to the region proximal to the epiphyseal line because the transition from bone to cartilage made BV/TV calculations distal to the epiphyseal line not possible<sup>32</sup>. Bone-implant contact (BIC) was not calculated due to the dilation of the implant removing the actual interface. Measurements of BIC through  $\mu$ CT were unreliable in a previous study<sup>33</sup>. Other architectural parameters were not evaluated as they are often correlated with the BV/TV and may result in a type I error of detecting a difference when there is not.

#### Histological staining

Femurs were dehydrated with ethanol, stripped of lipids with acetone and embedded in methacrylate resin (Technovit 7200 VLC, EXAKT, Oklahoma City, OK, US) under constant agitation via a stir bar in a vacuum desiccator after  $\mu$ CT scanning. Following infiltration, the specimens, secured in molds at each end of the implant with a custom fixture maintaining cranial-caudal orientation along the implant axis at the midline of the mold cavity, were fully embedded in methacrylate resin. The specimens were sectioned, mounted to slides and polished to a 25- $\mu$ m-thickness with a precision cutting/grinding system (EXAKT, Oklahoma City, OK, US)<sup>34</sup>. The sectioning plane was defined by the axes of the implant and femoral notch. The longitudinal sections were then stained with acid fuchsin for 3 minutes<sup>35</sup> and imaged through a 10x bright field lens with a two-second exposure on a microscope (Olympus BX51 with DP72 color camera). The resulting images (Figure 3) were evaluated for percent BV/TV within 250  $\mu$ m of the implant and BIC

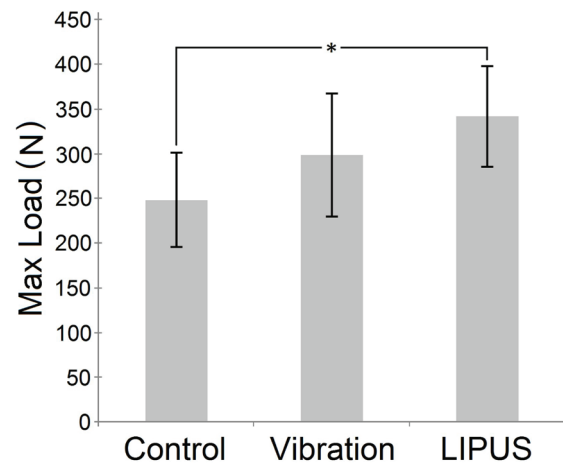


**Figure 4.** Mean and standard deviation of maximum load to failure of bone-implant interface of control, locally applied vibration and low-intensity pulsed ultrasound groups of 4 week study (N=10). \* notes significant difference.

using imaging software (Fiji, imagej.net) along the entire implant, excluding the distal 1.5-mm-long boss.

#### Statistical analysis

One-way analysis of variance with Holm-Sidak mean comparison testing for all outcome measures was performed to assess treatment effects using a statistical analysis program (SigmaPlot v11.0, Systat Software Inc, San Jose, CA).

## Results

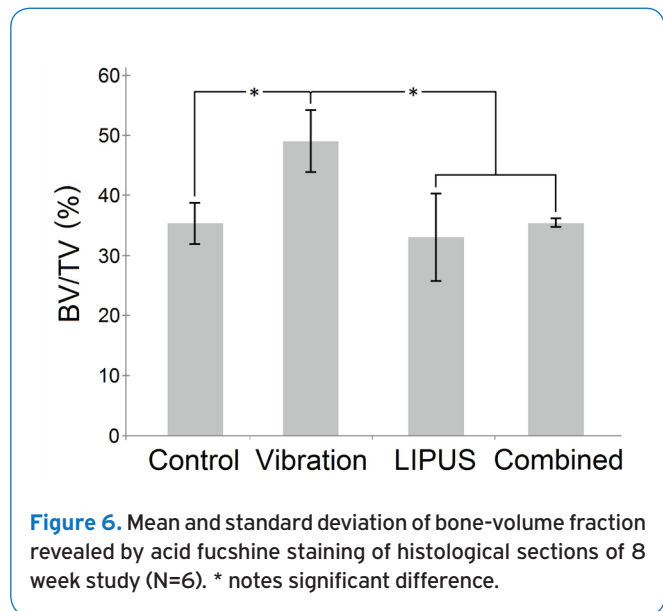
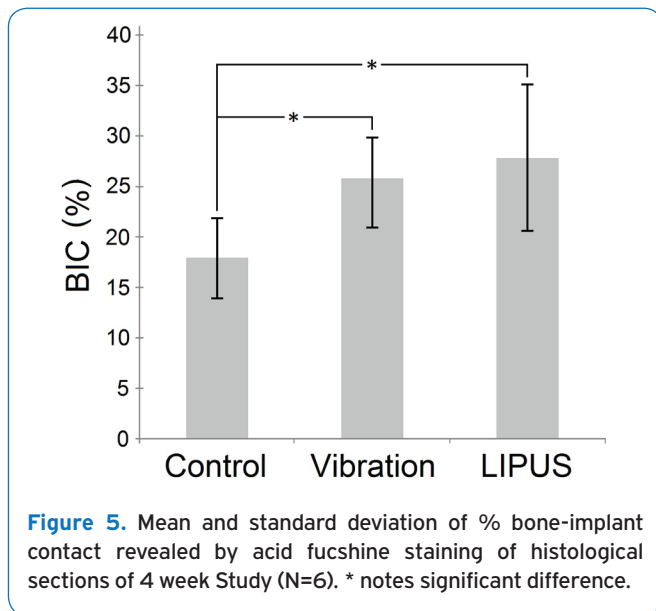
Radiographs confirmed the placement of bilateral implants and that no bone fractures occurred during implantation. No differences in weight change were noted between groups at either time point.

#### 4-week evaluations

Maximum pushout load of implants increased for both LIPUS and vibration groups relative to the control group

**Table 1.** Mechanical and biological outcomes (mean  $\pm$  SD) after surgical implantation of textured rods into rat femurs with adjunctive local vibration (Vibration), low-intensity pulsed ultrasound (LIPUS) or vibration and LIPUS (Combined). "a" differs significantly from "b" ( $P < 0.05$ ). "N" represents the number of specimens tested for each treatment group. NA = not available.

		Control	Vibration	LIPUS	Combined
4 Week (N=10)	Stiffness (N/mm)	1190 $\pm$ 128	1211 $\pm$ 92	1263 $\pm$ 60	NA
	Max Load (N)	248 $\pm$ 53 <sup>a</sup>	298 $\pm$ 69	341 $\pm$ 57 <sup>b</sup>	NA
	Energy (mJ)	29.8 $\pm$ 9.5 <sup>a</sup>	42.9 $\pm$ 17.3	52.0 $\pm$ 11.2 <sup>b</sup>	NA
8 Week (N=10)	Stiffness (N/mm)	1940 $\pm$ 149	1944 $\pm$ 362	2120 $\pm$ 268 <sup>b</sup>	1657 $\pm$ 411 <sup>a</sup>
	Max Load (N)	423 $\pm$ 52	433 $\pm$ 104	439 $\pm$ 101	437 $\pm$ 32
	Energy (mJ)	51.0 $\pm$ 10.5	55.7 $\pm$ 21.9	57.7 $\pm$ 25.3	70.0 $\pm$ 18.7
4 Week $\mu$ CT (N=8)	Prox. BV/TV	7.7 $\pm$ 1.9%	6.6 $\pm$ 2.3%	6.4 $\pm$ 1.7%	NA
	Dist. BV/TV	29.6 $\pm$ 5.9% <sup>a</sup>	34.7 $\pm$ 5.2%	38.7 $\pm$ 1.9% <sup>b</sup>	NA
8 Week $\mu$ CT (N=9)	Prox. BV/TV	6.6 $\pm$ 5.2%	5.6 $\pm$ 3.5%	4.9 $\pm$ 4.3%	3.8 $\pm$ 3.5%
	Dist. BV/TV	27.8 $\pm$ 8.4% <sup>a</sup>	36.0 $\pm$ 6.6% <sup>b</sup>	27.2 $\pm$ 3.6% <sup>a</sup>	30.2 $\pm$ 4.9%
4 Week Histology (N=6)	BV/TV	32.7 $\pm$ 4.1%	35.1 $\pm$ 5.8%	37.9 $\pm$ 4.4%	NA
	BIC	17.9 $\pm$ 4.1% <sup>a</sup>	25.4 $\pm$ 4.5% <sup>b</sup>	27.9 $\pm$ 7.3% <sup>b</sup>	NA
8 Week Histology (N=6)	BV/TV	35.3 $\pm$ 3.5% <sup>a</sup>	49.1 $\pm$ 5.3% <sup>b</sup>	33.0 $\pm$ 7.4% <sup>a</sup>	35.4 $\pm$ 0.8% <sup>a</sup>
	BIC	31.4 $\pm$ 5.7%	35.9 $\pm$ 13.6%	30.0 $\pm$ 3.9%	31.8 $\pm$ 1.3%



in the 4-week study (37.7% [ $P=0.002$ ] and 20.2% respectively, Figure 4) with the increase from vibration failing to reach statistical significance. Similarly, the energy to maximum load was increased by 74.5% for the LIPUS group relative to the control, while the vibration group was not found to differ from the control (Table 1). The stiffness of the bone-implant interface from the pushout test was not found to differ among any of the groups (Table 1).

The  $\mu$ CT evaluation demonstrated that LIPUS significantly (30.7% [ $P=0.003$ ]) improved peri-implant BV/TV in the metaphyseal (distal) region relative to the control group,

while the vibration group was not found to differ from the control (Table 1). In contrast, no group differences were found in the peri-implant BV/TV in the diaphyseal (proximal) region for the  $\mu$ CT evaluation.

For the histological evaluation, no group differences were detected in the peri-implant BV/TV (Table 1). However, the histological evaluation of BIC did find significant [ $P < 0.05$ ] improvements in bone ongrowth to the implant for both the LIPUS and vibration groups relative to the control (55.9% and 41.9% respectively, Figure 5).

### 8-week evaluations

Pushout testing at the 8-week time point revealed no individual treatment group differences relative to the control for the maximum pushout load, energy to maximum load, or stiffness (Table 1). Curiously, the combined LIPUS and vibration group was found to have significantly (21.8% [ $P=0.003$ ]) decreased stiffness relative to the LIPUS alone group.

The  $\mu$ CT evaluation at 8 weeks at the metaphyseal region found the vibration group to have significantly improved peri-implant bone volume relative to either the control or LIPUS alone group (29.5% and 32.4% respectively [ $P<0.01$ ]). In contrast, no group differences were found in diaphyseal (proximal) region (Table 1).

For the histological evaluation peri-implant bone volume of the vibration alone group was significantly improved relative to all the remaining groups (25.7% average [ $P<0.001$ ], Figure 6). However, the BIC by histological evaluation was not found to differ among the groups at 8 weeks (Table 1).

## Discussion

LIPUS has been shown to upregulate mRNAs involved in bone healing (alkaline phosphatase, osteocalcin, insulin-like growth factors and bone sialoprotein)<sup>36,37</sup> and have a metabolic impact during all phases of bone healing<sup>38</sup>. While prior LIPUS studies have shown increased bone formation around intramedullary implants, none have investigated the beneficial effects of LIPUS on intramedullary implant mechanical stability in animals including rats, rabbits and dogs<sup>22-24,39</sup>. This study demonstrates that LIPUS treatments result in accelerated bone healing and lead to improved osseointegration at 4 weeks with significantly increased axial load capabilities and energy to failure. These benefits are most likely a result of the increased bone surrounding the implant in the form of BV/TV seen through  $\mu$ CT and the BIC seen in histomorphometric evaluations of the acid fuchsin-stained specimens (Table 1). Interestingly, the therapeutic benefits to osseointegration were no longer detected after 8 weeks, possibly because the native biological bone healing process caught up, as seen in the histologic results in a prior study<sup>22</sup>. For the implantation model used in the current study, an upper implant mechanical stability limit may be reached earlier with the LIPUS treatment compared to no treatment. The observed hastening of the bone-implant mechanical stability indicates that LIPUS appears to be a therapeutic tool for accelerating bone ingrowth and patient rehabilitation.

LMHF vibration has been demonstrated as a successful treatment for fracture healing with several animal studies showing increased callus formation<sup>16,17</sup> and higher mineral content<sup>40-42</sup>. The dual limb local vibration stimulators of this study were tuned to deliver similar LMHF vibration to the implant site as an optimal WBV determined in a prior study. Histomorphometric evaluation revealed an increase in BIC by 4 weeks. Despite the improvement in BIC with vibration, the numerical increase in load to failure of the vibration group

at 4 weeks did not reach statistical significance. While the reason for this discrepancy is unclear; it may be that the newly formed bone in response to vibration is not fully mineralized or of lower quality such that significant improvements in mechanical stability are not realized. Later, at 8 weeks, vibration caused an increase in BV/TV as detected by  $\mu$ CT and histologic evaluations. However, similar to the 4-week point there was no difference in mechanical stability of the vibration group relative to the control group at 8 weeks. These findings confirm the marginal benefits to implant-bone mechanical stability resulting from vibration stimulation<sup>43-47</sup>. Nevertheless, vibration may aid in maintaining or increasing peri-implant bone volume during the rehabilitation period, while the bone is not fully loaded.

Combined treatment of LIPUS and locally applied vibration did not demonstrate an improved 8-week osseointegration. Contrary to expectations, combining LIPUS and vibration resulted in decreased bone-implant stiffness relative to the LIPUS only. Axial loads to failure, however, were not affected by the combination of LIPUS and vibration compared to LIPUS only. Experimentally, fibrous collagen tissue stiffness is two orders of magnitude lower than cancellous bone<sup>48</sup>. However, it is unclear whether the reduced bone-implant stiffness was due to fibrous encapsulation or to the presence of cancellous bone that had not fully mineralized.

This study had limitations. Reaching the apparent mechanical limits of the bone-implant interface around 4 weeks was not anticipated and, in an attempt, to reduce the number of animals used in this study, combined treatment effects were only investigated for osseointegration at 8 weeks. Because the mechanism of bone healing through vibration and LIPUS is not fully understood, a cumulative osseointegration benefit at 4 weeks with combined treatments of LIPUS and vibration may still be realized and should be investigated.

Also, the long-term mechanical or peri-implant bone benefits of the increased BV/TV and BIC seen at 8 weeks from locally applied vibration treatments were not investigated. Whether these increases persist after the end of the treatment period and what their long-term effects are on mechanical stability as the newly formed peri-implant bone matures should be investigated.

As the primary target for percutaneous osseointegrated implants are healthy and active trauma amputees<sup>2,49</sup>, we utilized a retired breeder female rat model to simulate an adult bone model. Female animals were used to allow comparison to ovariectomized (OVX) rat model studies that have been utilized to study postmenopausal osteoporosis and the effects of vibration on preventing such bone loss. However, we felt the OVX model was not a necessary model for our target clinical population because we did not intend to study the response of osteoporotic bone to therapy.

Finally, the AM implants were designed to fit a range of intramedullary canals without concern for the axial orientation of the implant during surgical placement to facilitate mass production and ease of surgery. A key benefit of using AM implants is that they can be customized to

match patient specific anatomy. In a clinical environment, the implant could be designed to more closely interface with the endosteal surface which may affect the bone healing response to treatments and the resulting mechanical stability as studies suggested vibration primarily affects cancellous bone and the endosteal surfaces by acting on osteoblasts or precursor cells<sup>50</sup>.

## Conclusion

Vibration demonstrated improved peri-implant bone volume with increased BIC. LIPUS was superior to vibration for accelerating osseointegration at 4 weeks through increased axial force for bone-implant interface failure. LIPUS enhances early bone ongrowth potentially stabilizing future constructs allowing for accelerated implant loading with a reduced likelihood of fibrous ingrowth. LIPUS can be used as a therapeutic tool for possibly reducing the rehabilitation period of direct skeletal limb prostheses. The osseointegration benefits of LIPUS were no longer present at 8 weeks as the native biological ingrowth process appeared to catch up. However, vibration therapy continued to increase the amount of bone around the implant without affecting the mechanical properties of the bone-implant interface. Vibration has demonstrated its therapeutic benefits for increasing bone adjacent to the implant.

## Acknowledgements

*Funding/Support:* This work was supported by the National Science Foundation under Award Number CBET-1441636. Any opinions, findings, and conclusions or recommendations expressed in this material are those of the authors and do not necessarily reflect the views of the National Science Foundation.

*Additional Contributions:* We thank the Small Animal Imaging Facility at the UNC Biomedical Imaging Research Center for providing the  $\mu$ CT imaging service, and the imaging core is supported in part by an NCI cancer core grant, P30-CA016086-40. Thanks goes to Laurence Dahners, MD for his guidance on surgical techniques for the intramedullary rodent model. Thanks also goes to Stephen Kallianos for his many hours of animal handling in the first cohort. Gratitude also goes to Bioventus (Durham, NC) for loaning the Exogen LIPUS units and donating the ultrasound gel used during the study. Appreciation for instruction and use of the EXAKT grinding and cutting system goes to the Histology laboratory, Department of Population Health and Pathobiology, College of Veterinary Medicine, NCSU.

*Author Contribution:* David Ruppert – Helped design and orchestrate study. Organized and performed experiments, collected and analyzed data, evaluated results, and authored publications and verifies the integrity of the data analysis. Ola Harryson – Spearheaded study design. Helped orchestrate the study, participated in data evaluation and edited manuscript. Denis Marcellin-Little – Helped design and orchestrate the study, participated in data evaluation and edited manuscript. Seth Bollenbecker – Assisted in all experiments, collection of data and edited manuscript. Paul Weinhold – Supervised all efforts, and spearheaded the experimental design, results analysis, and manuscript preparation.

## References

- Ziegler-Graham K, MacKenzie EJ, Ephraim PL, Trivison TG, Brookmeyer R. Estimating the prevalence of limb loss in the United States: 2005 to 2050. *Arch Phys Med Rehabil* 2008;89(3):422-429.
- Hagberg K, Brånemark R. One hundred patients treated with osseointegrated transfemoral amputation prostheses-rehabilitation perspective. *J Rehabil Res Dev* 2009;46(3):331-344.
- Sullivan J, Uden M, Robinson K, Sooriakumaran S. Rehabilitation of the trans-femoral amputee with an osseointegrated prosthesis: The United Kingdom experience. *Prosthet Orthot Int* 2003;27(2):114-120.
- Brånemark R, Brånemark PI, Rydevik B, Myers RR. Osseointegration in skeletal reconstruction and rehabilitation: A review. *J Rehabil Res Dev* 2001;38(2):175-181.
- Pezzin LE, Dillingham TR, MacKenzie EJ. Rehabilitation and the long-term outcomes of persons with trauma-related amputations. *Arch Phys Med Rehabil* 2000;81(3):292-300.
- Albrektsson T, Brånemark P, Hansson H, Lindström J. Osseointegrated titanium implants: Requirements for ensuring a long-lasting, direct bone-to-implant anchorage in man. *Acta Orthop Scand* 1981; 52(2):155-170.
- Chausu G, Chausu S, Tzohar A, Dayan D. Immediate loading of single-tooth implants: Immediate versus non-immediate implantation. A clinical report. *Int J Oral Maxillofac Implants* 2001;16(2):267-272.
- Jeyapalina S, Beck JP, Bachus KN, Williams DL, Bloebaum RD. Efficacy of a porous-structured titanium subdermal barrier for preventing infection in percutaneous osseointegrated prostheses. *J Orthop Res* 2012;30(8):1304-1311.
- Raphel J, Holodniy M, Goodman SB, Heilshorn SC. Multifunctional coatings to simultaneously promote osseointegration and prevent infection of orthopaedic implants. *Biomaterials* 2016;84:301-314.
- Southam J, Selwyn P. Structural changes around screws used in the treatment of fractured human mandibles. *Br J Oral Surg* 1970;8(3):211-221.
- Szmukler-Moncler S, Salama H, Reingewirtz Y, Dubruille J. Timing of loading and effect of micromotion on bone-dental implant interface: Review of experimental literature. *J Biomed Mater Res*. 1998; 43(2): 192-203.
- Rao PL, Gill A. Primary stability: The password of implant integration. *J Dent Implant* 2012;2(2):103-109.
- Simon U, Augat P, Ignatius A, Claes L. Influence of the stiffness of bone defect implants on the mechanical conditions at the interface - a finite element analysis with contact. *J Biomech* 2003;36(8):1079-1086.
- Büchler P, Pioletti DP, Rakotomanana L. Biphasic constitutive laws for biological interface evolution. *Biomech Model Mechanobiol* 2003;1(4):239-249.
- Brånemark R, Berlin O, Hagberg K, Bergh P, Gunterberg B, Rydevik B. A novel osseointegrated percutaneous prosthetic system for the treatment of patients with transfemoral amputation. *Bone Joint J* 2014;96(1):106-113.



16. Wolf S, Augat P, Eckert-Hübner K, Laule A, Krischak GD, Claes LE. Effects of high-frequency, low-magnitude mechanical stimulus on bone healing. *Clin Orthop* 2001; 385:192-198.
17. Usui Y, Zerwekh JE, Vanharanta H, Ashman RB, Mooney V. Different effects of mechanical vibration on bone ingrowth into porous hydroxyapatite and fracture healing in a rabbit model. *J Orthop Res* 1989;7(4):559-567.
18. Pounder NM, Harrison AJ. Low intensity pulsed ultrasound for fracture healing: A review of the clinical evidence and the associated biological mechanism of action. *Ultrasonics* 2008;48(4):330-338.
19. Ruppert D, Harrysson O, Marcellin-Little D, Dahners L, Weinhold P. Osseointegration of EBM textured and threaded implants through whole body vibration. ORS Annual Meeting, Orlando, FL. 2016, paper no. 0055.
20. Ogawa T, Zhang X, Naert I, et al. The effect of whole-body vibration on peri-implant bone healing in rats. *Clin Oral Implants Res* 2011;22(3):302-307.
21. Rubin C, Pope M, Fritton C, Magnusson M, Hansson T, McLeod K. Transmissibility of 15-hertz to 35-hertz vibrations to the human hip and lumbar spine: determining the physiologic feasibility of delivering low-level anabolic mechanical stimuli to skeletal regions at greatest risk of fracture because of osteoporosis. *Spine* 2003;28(23):2621-2627.
22. Tanzer M, Harvey E, Kay A, Morton P, Bobyn J. Effect of noninvasive low intensity ultrasound on bone growth into porous-coated implants. *J Orthop Res* 1996;14(6): 901-906.
23. Ustun Y, Erdogan O, Kurkcu M, Akova T, Damlar İ. Effects of low-intensity pulsed ultrasound on dental implant osseointegration: A preliminary report. *Eur J Dent* 2008;2:254-262.
24. Tanzer M, Kantor S, Bobyn J. Enhancement of bone growth into porous intramedullary implants using non-invasive low intensity ultrasound. *J Ortho Res* 2001; 19(2):195-199.
25. Chen B, Li Y, Xie D, Yang X. Low-magnitude high-frequency loading via whole body vibration enhances bone-implant osseointegration in ovariectomized rats. *J Orthop Res* 2012;30(5):733-739.
26. Ruppert D, Harrysson O, Marcellin-Little D, Dahners L, Abumoussa S, Weinhold P. Osseointegration of coarse and fine textured implants manufactured by electron beam melting and direct metal laser sintering. *3D Print Addit Manuf* 2017;4(2):91-97.
27. Alghamdi HS, van den Beucken, Jeroen JJP, Jansen JA. Osteoporotic rat models for evaluation of osseointegration of bone implants. *Tissue Eng Part C Methods* 2013;20(6):493-505.
28. De Ranieri A, Viridi A, Kuroda S, Healy K, Hallab N, Sumner D. Saline irrigation does not affect bone formation or fixation strength of hydroxyapatite/tricalcium phosphate-coated implants in a rat model. *J Biomed Mater Res B* 2005;74(2):712-717.
29. Ysander M, Branemark R, Olmarker K, Myers RR. Intramedullary osseointegration: Development of a rodent model and study of histology and neuropeptide changes around titanium implants. *J Rehabil Res Dev* 2001;38(2):183-190.
30. Pecoraro N, Reyes F, Gomez F, Bhargava A, Dallman MF. Chronic stress promotes palatable feeding, which reduces signs of stress: Feedforward and feedback effects of chronic stress. *Endocrinology* 2004;145(8): 3754-3762.
31. Ely DR, Dapper V, Marasca J, et al. Effect of restraint stress on feeding behavior of rats. *Physiol Behav* 1997; 61(3):395-398.
32. Viridi AS, Liu M, Sena K, et al. Sclerostin antibody increases bone volume and enhances implant fixation in a rat model. *J Bone Joint Surg Am* 2012; 94(18):1670-1680.
33. Liu S, Broucek J, Viridi AS, Sumner DR. Limitations of using micro-computed tomography to predict bone-implant contact and mechanical fixation. *J Microsc* 2012;245(1):34-42.
34. Donath K. Preparation of histologic sections. Norderstedt: EXAKT-Kulzer; 1988.
35. Piattelli A, Misch C, Pontes A, Iezzi G, Scarano A, Degidi M. Dental implant surfaces: A review. In: Contemporary implant dentistry. 2<sup>nd</sup> ed. Missouri: Mosby; 2008:612-615.
36. Warden SJ, Favaloro JM, Bennell KL, et al. Low-intensity pulsed ultrasound stimulates a bone-forming response in UMR-106 cells. *Biochem Biophys Res Commun* 2001;286(3):443-450.
37. Naruse K, Mikuni-Takagaki Y, Azuma Y, et al. Anabolic response of mouse bone-marrow-derived stromal cell clone ST2 cells to low-intensity pulsed ultrasound. *Biochem Biophys Res Commun* 2000;268(1):216-220.
38. Azuma Y, Ito M, Harada Y, Takagi H, Ohta T, Jingushi S. Low-Intensity pulsed ultrasound accelerates rat femoral fracture healing by acting on the various cellular reactions in the fracture callus. *J Bone Miner Res* 2001; 16(4):671-680.
39. Liu Q, Liu X, Liu B, Hu K, Zhou X, Ding Y. The effect of low-intensity pulsed ultrasound on the osseointegration of titanium dental implants. *Br J Oral Maxillofac Surg* 2012;50(3):244-250.
40. Garman R, Gaudette G, Donahue L, Rubin C, Judex S. Low-level accelerations applied in the absence of weight bearing can enhance trabecular bone formation. *J Orthop Res* 2007;25(6):732-740.
41. Goodship AE, Lawes TJ, Rubin CT. Low-magnitude high-frequency mechanical signals accelerate and augment endochondral bone repair: Preliminary evidence of efficacy. *J Orthop Res* 2009;27(7):922-930.
42. Stuermer EK, Komrakova M, Werner C, et al. Musculoskeletal response to whole-body vibration during fracture healing in intact and ovariectomized rats. *Calcif Tissue Int* 2010;87(2):168-180.
43. Judex S, Lei X, Han D, Rubin C. Low-magnitude mechanical signals that stimulate bone formation in

- the ovariectomized rat are dependent on the applied frequency but not on the strain magnitude. *J Biomech* 2007;40(6):1333-1339.
44. Christiansen BA, Silva MJ. The effect of varying magnitudes of whole-body vibration on several skeletal sites in mice. *Ann Biomed Eng* 2006;34(7):1149-1156.
  45. Rubin C, Turner A, Mallinckrodt C, Jerome C, McLeod K, Bain S. Mechanical strain, induced noninvasively in the high-frequency domain, is anabolic to cancellous bone, but not cortical bone. *Bone* 2002;30(3):445-452.
  46. Rubin C, Turner AS, Bain S, Mallinckrodt C, McLeod K. Anabolism: Low mechanical signals strengthen long bones. *Nature* 2001;412(6847):603-604.
  47. Hwang SJ, Lublinsky S, Seo Y, Kim IS, Judex S. Extremely small-magnitude accelerations enhance bone regeneration: A preliminary study. *Clin Orthop* 2009;467(4):1083-1091.
  48. Hori R, Lewis J. Mechanical properties of the fibrous tissue found at the bone-cement interface following total joint replacement. *J Biomed Mater Res A* 1982; 16(6):911-927.
  49. Usufzy P. Rare procedure in US promises amputee quality of life. <https://www.reviewjournal.com/local/local-las-vegas/rare-procedure-in-us-promises-amputee-quality-of-life/>. Updated 2016. Accessed 01/28, 2019.
  50. Rubin CT, Sommerfeldt DW, Judex S, Qin Y. Inhibition of osteopenia by low magnitude, high-frequency mechanical stimuli. *Drug Discov Today* 2001;6(16): 848-858.